Analyst

All-Electrical Antibiotic Susceptibility and Resistance Profiling of Electrogenic Pseudomonas aeruginosa

Journal:	*Analyst*
Manuscript ID	AN-ART-03-2023-000401.R1
Article Type:	Paper
Date Submitted by the Author:	04-May-2023
Complete List of Authors:	Rafiee, Zahra; Binghamton University Choi, Seokheun; Binghamton University, Dept of Electrical & Computer Engineering

All-Electrical Antibiotic Susceptibility and Resistance Profiling of Electrogenic *Pseudomonas aeruginosa*

*Zahra Rafiee[1], and Seokheun Choi[1,2]**

[1]Bioelectronics & Microsystems Laboratory, Department of Electrical & Computer Engineering, State University of New York at Binghamton, Binghamton, New York, 13902, USA

[2]Center for Research in Advanced Sensing Technologies & Environmental Sustainability, State University of New York at Binghamton, Binghamton, New York, 13902, USA

*Corresponding Author. Email: sechoi@binghamton.edu

Abstract: There is a pressing need for evidence-based, non-surgical therapy guidance for biofilm-based infections. Conventional phenotypic or genotypic or emerging antibiotic susceptibility testing (AST) techniques cannot provide clinically relevant guidelines and widely adaptable stewardship for effective biofilm treatment because they are mainly limited to planktonic bacteria and suffer from many technical and operational challenges. Here, we created an all-electrical, reliable, rapid AST device to monitor antibiotic efficacy in bacterial biofilms that can be practically translatable to clinical settings and industrial antibiotic developments. The electrons metabolically produced by a *Pseudomonas aeruginosa* biofilm provided a strong signal for monitoring bacterial growth and treatment efficacy while a 3-D paper-based culturing platform provided a new strategy for rapid biofilm formation through capillary action. When antibiotics are effective against the pathogenic biofilm, their metabolic activities are inhibited, decreasing their electron transfer reactions. The changes in electrical outputs can be measured to assess the treatment effectiveness against pathogenic biofilms. Within 100 minutes, our six-well AST device successfully distinguished antibiotic-susceptible and -resistant *P. aeruginosa* biofilms,

provided a quantifiable minimum inhibitory concentration (MIC) of antibiotics, and characterized the bacterial antibiotic action mechanisms.

Keywords: Antibacterial sustainability test (AST); Electrogenic pathogens; Extracellular electron transfer (EET); Minimum inhibitory concentration (MIC); Paper-based culturing platforms; Antibiotic mechanism of action

1. Introduction

More than half of all humans who have ever existed on earth have died of infectious diseases.[1] Even in the 21st century with significant technological developments in sanitation and human health, pathogenic diseases are the major leading cause of death globally.[2] Ridiculously, we humans are plagued by only about 1,400 human pathogens which is much less than 1% of all types of microorganisms living on earth.[1,3] Undoubtedly, antibiotics are one of the greatest discoveries of the 20th century, revolutionizing the treatment of diseases and saving millions of lives.[4] However, we are now approaching a "post-antibiotic era" in which existing antibiotics lose effectiveness because pathogens readily develop resistance by avoiding the action of the antibiotics.[5] The overuse or misuse of empiric antibiotics promotes antibiotic resistance.[6] Even worse, the discovery and development of new antibiotics are being discouraged because of laborious, expensive, and time-consuming procedures that lead to an extremely low return on investment in pharmaceutical industries.[7] Since 2000, only 12 new antibiotics have been added while most big pharmaceutical companies have closed their research programs for new antibiotic developments.[7,8]

Antibiotic susceptibility testing (AST) has been the most effective method to promote appropriate antibiotic use and slow the spread of antibiotic resistance.[9] Furthermore, AST plays a pivotal role in the discovery and development of new antibiotics.[7,10] Unfortunately,

conventional phenotypic ASTs based on slow bacterial growth monitoring with antibiotics are not suitable for rapid clinical or analytical decision-making.[11,12] Genotypic ASTs are quite limited as well because the techniques require knowledge of specific resistance genes and expensive equipment-intensive procedures.[13,14] Genotypic ASTs are widely used to identify the antibiotic mechanism of action for new antibiotic developments.[15] Phenotypic observations, which do not rely on genetic modifications, could provide much reliable quantitative understanding of a new antibiotic's effectiveness. However, the state-of-the-art does not provide cost-effective, *in situ*, and real-time phenotypic profiling of antibiotic-susceptible and resistant bacteria. Even emerging techniques combining phenotypic and genotypic ASTs cannot provide real-time profiling of antibiotic susceptibility and resistance especially in bacterial colonies and biofilms.[16,17] Usually, bacteria exist as structurally and functionally complex clusters that can develop many defense strategies that cannot be replicated with the planktonic forms used in the experimental setups in laboratories.[18] All existing techniques cannot replicate a real clinical situation with cluster-associated infections.

Here, we provide an all-electrical, cost-effective, *in situ*, real-time, rapid profiling approach for antibiotic susceptibility and resistance in bacterial biofilms. The approach can be practically translatable to clinical settings and industrial antibiotic developments (Figure 1). Bacterial viability, growth, metabolism, and treatment efficacy against the biofilm are sensitively and continuously assessed by monitoring the collective extracellular electron transfer (EET) generated from the biofilm, which are rapidly formed in a paper-based platform. Electrically monitoring the bacterial EET can be a simple but powerful and rapid method to determine the antibiotic effectiveness and even characterize the antibiotic mechanism of action (Figure 1a). Additionally, the electrical sensing platform is very

attractive because of its miniature size, integrability with electrical components, and simple operation for portable and point-of-care diagnostic and analytical applications in a cost-effective way. The EET profiles successfully classify antibiotic-susceptible and -resistant bacteria, and precisely determine the minimum inhibitory concentration (MIC) of antibiotics required to prevent the growth of antibiotic-susceptible bacteria. Moreover, our approach continuously monitors the antibiotic mechanism with different action modes. The paper-based culture platform provides a 3-D porous architecture that can mimic the host environment and enable rapid biofilm formation through capillary force (Figure 1b). Very recently, we successfully demonstrated that the EET profiles from the bacterial biofilm in the paper-based culturing platform had been sensitively responding to the antibiotics.[19,20] However, the reports failed to describe how the EET outputs can qualify as a real AST method that identifies antibiotic-susceptible and -resistant bacteria and how the outputs can innovatively identify the antibiotic mechanisms of action. In this work, we show how practically the bacterial EET on the paper-based bioelectrochemical system can be used to monitor antibiotic efficacy, quantify the MIC values, and provide mechanistic insights into antibiotic action. Our EET-based AST approach will provide clinically relevant therapeutic guidance for biofilm-associated infections and widely adaptable techniques to explore the antibiotic mechanism of action for new antibiotic discoveries and developments.

2. Results and discussion

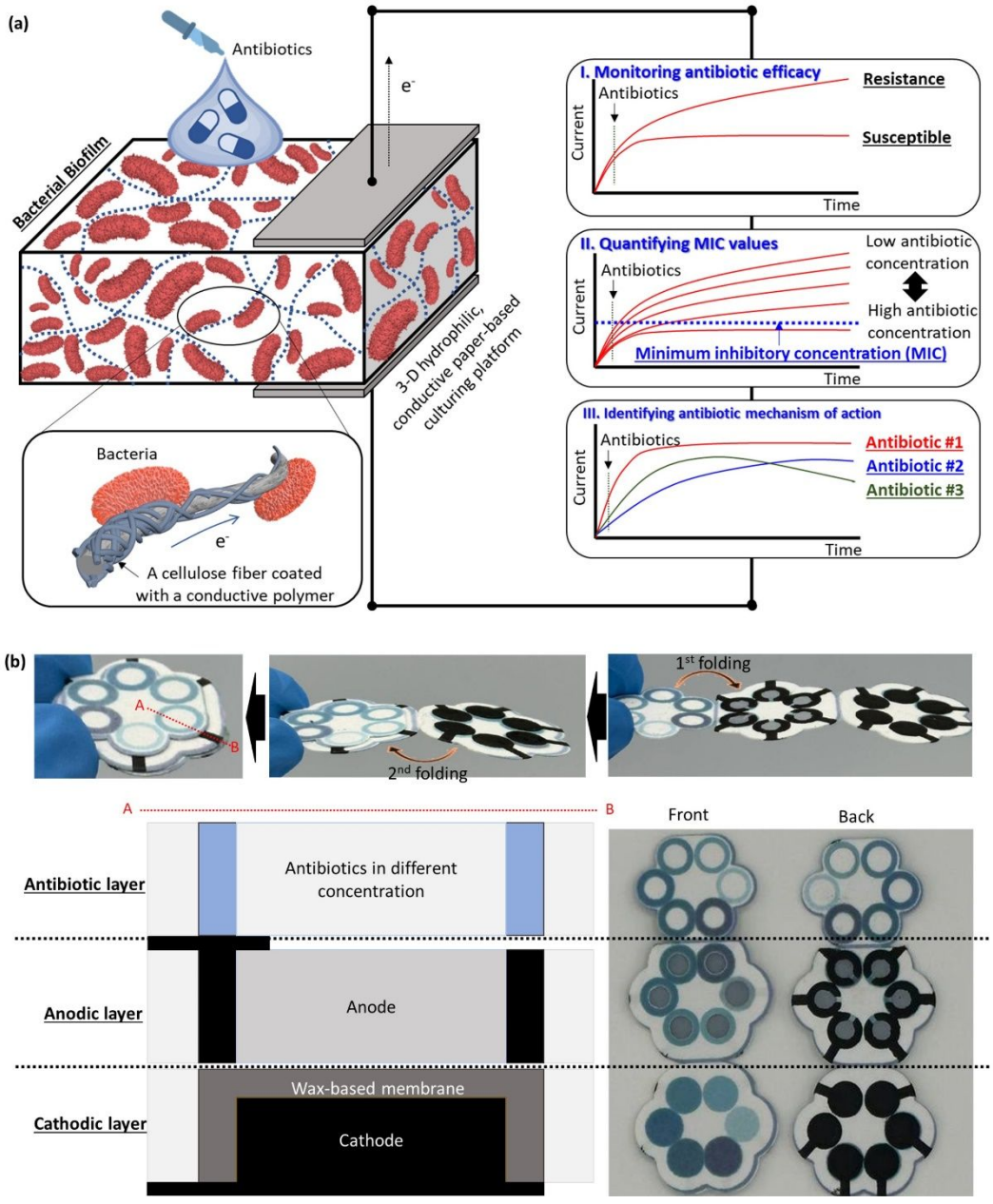

Figure 1. (a) A conceptual illustration of our EET-based AST device developed on a paper culturing platform. Our all-electrical rapid device monitors antibiotic efficacy, quantifies the MIC values, and provides mechanistic insights into antibiotic action in pathogenic biofilms. (b) The 3-D device is constructed by the origami folding of the 2-D sheet into three functional layers: antibiotic, anodic, and cathodic, which has a wax-based ion-exchange membrane. When the pathogenic samples are introduced through the antibiotic layer, the cells are transfered down to the anodic layer along with the pre-loaded antibiotics. The differrent bacerial and antibotic concentrations will generate different electricity profiles. The paper's capillary force enables the rapid formation of bacterial colonies.

2.1 Bacteria, device design and operation. Bacterial respiration produces indispensable energy to power cellular growth, maintenance, and reproduction.[21] Respiration requires organic fuel and an electron acceptor and generates electrons and protons from a series of chemical redox reactions by converting the fuel to energy in the form of adenosine triphosphate (ATP). Typically, microorganisms use oxygen as the final electron acceptor in the cellular electron transport chain to produce the proton gradient for ATP synthesis. Electrogenic bacteria are a particular species of microorganisms that can respire by exchanging electrons with external electrodes without oxygen, leading to electricity generation.[22] This extraordinary electron pathway is known as EET and has been harnessed in an engineered bioelectrochemical system, named a microbial fuel cell, for power generation.[23] The system consists of an anode, ion-exchange membrane, and cathode. When bacteria break down organic fuel, cellular respiration transfers electrons to the anode. The electrons move to the cathode along an external circuit while the generated protons flow to the cathode through the ion-exchange membrane, maintaining the electroneutrality of the system. Because the resultant bacterial electricity represents the degree of metabolic activity, the microbial fuel cell has been successfully demonstrated as a sensor to monitor toxicity in the environment.[23] In particular, the microbial fuel cell has been proposed as the next viable AST technology as the bacterial metabolism and their EET can be significantly affected by their susceptibility and resistivity to antibiotics.[19,20,23] Moreover, many pathogens are electrogenic, and more and more pathogens have shown weak electrogenic capabilities.[24] Such pathogens include *Enterococcus faecalis, Klebsiella variicola, Listeria monocytogenes,* and *Pseudomonas aeruginosa*. Although bacterial EET-based ASTs have been demonstrated electrochemically with a potentiostat[25] or electrically in a microbial fuel cell[19,20], quantifying the signal of those weak electrogenes and establishing their medical

relevance as a reliable AST technique is by far the most challenging part to approach. Especially, advances in this domain require establishing *in vitro* biofilm models that can represent 3-D clinical infections.

Here, *Pseudomonas aeruginosa* was selected as a model weak electrogenic pathogen. Our previous paper-based platforms for microbial cultivation[26] and paper-based microbial fuel cells[27] for sensing were revolutionarily changed for innovative AST in biofilm. Three hexagonal-shaped tabs prepared on a 2-D paper sheet developed a 3-D functional device by folding the paper twice. Each tab had six units that allowed high-throughput ASTs. The top tab was prepared with different concentrations of antibiotics and then air-dried before use. The middle paper tab to inoculate the bacterial sample was engineered with a conductive polymer, poly(3,4-ethylened ioxythiophene):polystyrene sulfonate (PEDOT:PSS) to allow the bacterial electrons to flow and effectively be measured. The bottom tab had a wax-based ion-exchange membrane for proton movement internally and a cathode for finalizing the reduction process of the system by combining the electrons and the protons. By folding, the middle and bottom tabs formed the microbial fuel cell while the complete AST device was finally realized with the top antibiotic layer. When the bacterial sample was introduced into the top layer, the paper's strong capillary force enabled the sample to be adsorbed and mixed with the pre-loaded antibiotics, followed by flowing to the anodic layer. By varying the concentrations of bacteria in the sample, we could test the antibiotic effectiveness against engineered biofilm models. Because the paper's fiber network developed micro-pores (~ 10 μm), the bacterial cells of ~ 2 μm size could freely move through the 3-D paper matrix. The bacterial cells attached themselves to the paper fibers to form the biofilm while the antibiotics influenced the bacterial metabolic activities. Previously, our group had comprehensively explored the biofilm formation in papers, demonstrating fast

accumulation and acclimation of the bacteria.[19,26] Paper as a substrate provides strong mechanical support for rapidly and controllably constructing a 3-D biofilm. Our microbial fuel cell monitored the biofilm growth in the presence of antibiotics, allowing *in situ* and real-time phenotypic screening with direct clinical and therapeutic relevance. While it has been straightforward to perform the direct measurement of electrical outputs from strong electrogenes such as *Geobacter sulfurreducens* and *Shewanella oneidensis*, it is substantially challenging to capture the signal of the weak electrogene, *P. aeruginosa*.[24] To improve a signal-to-noise ratio for sensitive AST with *P. aeruginosa*, we monitored the accumulated power continuously generated from the bacterial EET. This accumulated output power through time is defined as energy, "E", as described in the following,

$$E = \sum_0^T P.\Delta t \qquad (1)$$

where P is the output power measured from the device at time t, and T is the total accumulated time in seconds.[19,20] With the accumulation of electrical outputs through the bacterial EET, the AST device even with low bacterial concentrations demonstrates distinguishable antibiotic effectiveness. The limit of detection (LOD) of our sensor goes down to a lower level of 0.1 OD_{600} which is equivalent to a 0.5 McFarland standard.

2.2 Rapid differentiation of susceptible vs. resistant bacteria. By continuously monitoring the energy produced from the bacterial EET activities, we assessed susceptible and resistant *P. aeruginosa* to three antibiotics, gentamicin (GEM), ciprofloxacin (CIP), and ampicillin (AMP) (Figures 2, 3, and 4). While the gold standard broth microdilution (BMD) AST method uses a low bacterial concentration of 0.001 optical density at 600 nm (OD_{600}) in a planktonic form,[28] we tested three samples having a higher concentration of

0.1, 0.5, and 1.0 OD_{600} to form multiple biofilms over the paper-based culturing platform and evaluate the antibiotic efficacy against clinically relevant biofilms. Based on our previous report, even the small bacterial concentration of 0.1 OD_{600} (corresponding to 10^8 CFU/ml and the 0.5 McFarland turbidity standard) had readily and rapidly formed densely packed bacterial colonies in the 3-D porous cellulose structure while the antibiotic substances were effectively delivered to the individual cells in the biofilm.[19] The energy curves were obtained by subtracting the bacteria-free aseptic control from the bacterial sample to avoid abiotic noises and environmental interferences. All experiments were repeated at least three times and their standard deviations were plotted as a shaded area. Once the bacterial sample was introduced, we waited for 30 minutes to allow it to be absorbed by the paper, mixed with the pre-loaded antibiotics, and transported to the anodic layer to form a biofilm. Then, the energy was constantly measured for 4000 seconds (~ 67 minutes). While bacterial metabolism and reproduction (c.f. an average doubling time of *P. aeruginosa* is about 30 minutes in a Luria Broth (LB) medium) were carried out, the energy from the bacterial EET was continuously increased but never saturated within 4000 seconds in the absence of antibiotics (Figures 2, 3, and 4). This indicates that 5μL of each anodic chamber was not fully saturated within that time duration by multiplication of the bacterial samples with 0.1, 0.5, and 1.0 OD_{600}. Our previous report showed that 2.5 OD_{600} was able to saturate the volume of that chamber.[19] When the selected antibiotic is effective, bacterial metabolic activities, growth, and reproduction are inhibited and their energy output reaches a plateau. Therefore, bacterial susceptibility and resistance to antibiotics can be readily differentiated depending on whether plateaus are observed.

First, GEM-susceptible and -resistant *P. aeruginosa* were investigated (Figure 2 and Tables S1 and S2). Overall, as the concentration of the bacteria increased, the energy value

was significantly raised because of the increased electricity generation from more cells. When the sample concentration is low at 0.1 OD_{600}, the plateau was observed even with 2μg/mL of GEM, representing "susceptible" while the standard BMD using the much smaller concentration shows "resistant" with that concentration. This result demonstrates that our 3-D culturing platform allows more effective delivery of antibiotics. The increasing GEM concentration moved up the onset time of plateaus while reducing the energy output. With the sample concentration of 0.5 OD_{600}, 2μg/mL of GEM was not effective. The sample was susceptible to its 4μg/ml and above at a much more delayed onset time than the 0.1 OD_{600}. Samples at 1.0 OD_{600} show "resistant" to all selected concentrations of GEM, showing that antibiotic efficacy significantly decreased with increasing bacterial numbers in a biofilm. All GEM-resistant *P. aeruginosa* did not generate any flat regions of the energy outputs.

For CIP-susceptible *P. aeruginosa*, both 0.1 and 0.5 OD_{600} samples show "susceptible" with all selected CIP concentrations (Figure 3 and Tables S3 and S4). However, the sample with higher cell density at 1.0 OD_{600} shows "resistant" to the antibiotic. CIP-resistant *P. aeruginosa* were all resistant regardless of cell concentrations.

Because *P. aeruginosa* is usually AMP resistant,[29] only 100μg/mL of AMP was weakly effective against the low concentration of *P. aeruginosa* at 0.1 OD_{600} (Figure 4 and Tables S5 and S6). AMP-susceptible and -resistant *P. aeruginosa* at the highest concentration show negligible output difference.

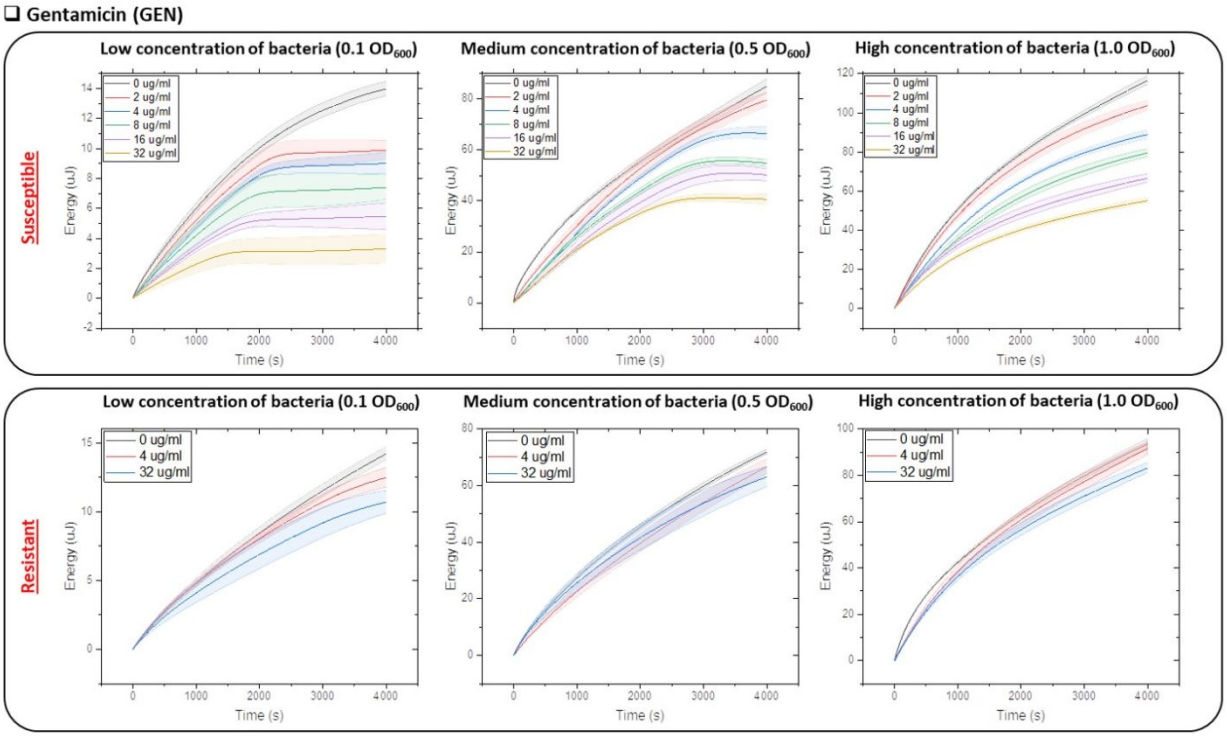

Figure 2. Gentamicin effectiveness to susceptiable and resistant *P. aeruginosa.* Electrical energy generated from the EET-based AST is continuously monitored with respect to inoculum and antibiotic concentrations. The energy is measured in micro-jules with three different bacterial concentrations; 0.1 OD_{600}, 0.5 OD_{600}, and 1.0 OD_{600}.

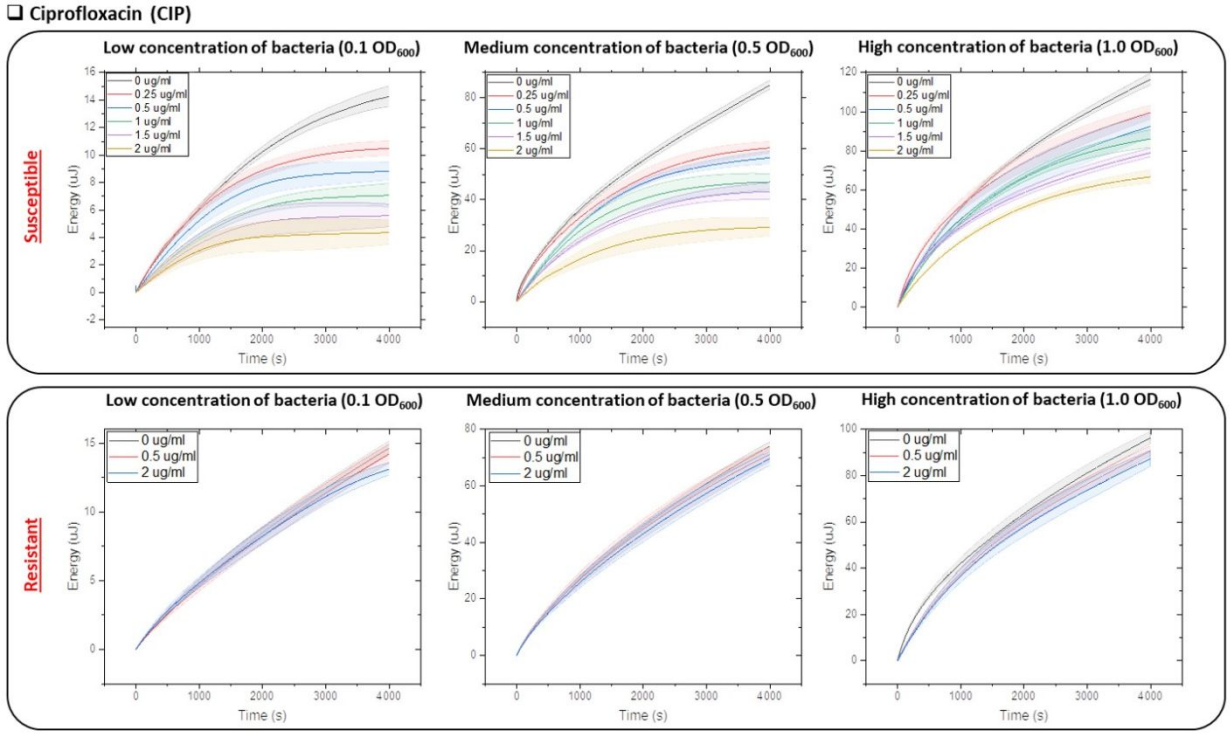

Figure 3. Ciprofloxacin effectiveness to susceptiable and resistant *P. aeruginosa.* Electrical energy generated from the EET-based AST is continuously monitored with respect to inoculum and antibiotic concentrations. The energy is measured in micro-jules with three different bacterial concentrations; 0.1 OD_{600}, 0.5 OD_{600}, and 1.0 OD_{600}.

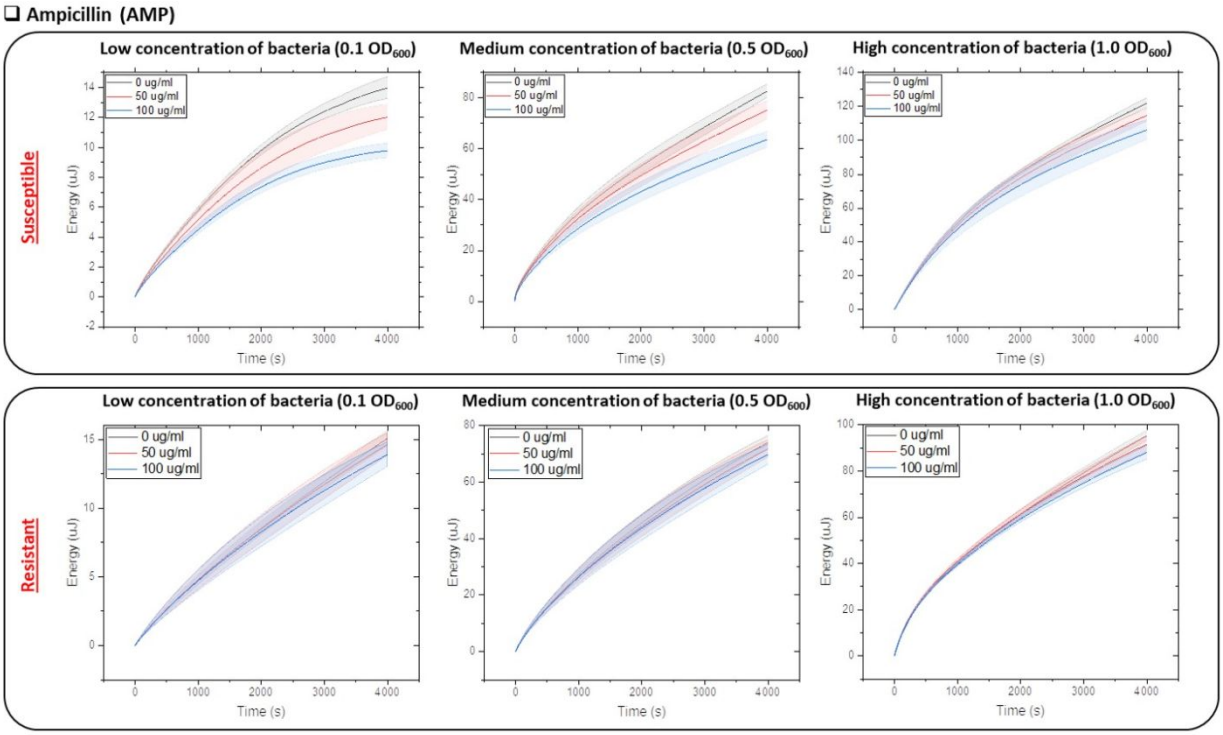

Figure 4. Ampicillin effectiveness to susceptiable and resistant *P. aeruginosa.* Electrical energy generated from the EET-based AST is continuously monitored with respect to inoculum and antibiotic concentrations. The energy is measured in micro-jules with three different bacterial concentrations; 0.1 OD_{600}, 0.5 OD_{600}, and 1.0 OD_{600}.

All results demonstrate that our EET-based AST device with the paper culturing platform clearly distinguishes susceptible and resistant *P. aeruginosa* in their biofilms.

2.3 Determination of minimum inhibitory concentrations (MICs). Fast and easy determination of antibiotic susceptibility and resistance against pathogenic biofilms will improve antibiotic stewardship and reduce antimicrobial resistance by choosing the right antibiotics. However, the MIC information for the exact antibiotic dose will be required to effectively treat a biofilm infection and better control the spread of the resistance. The MIC is the lowest antibiotic concentration that inhibits the visual growth of a pathogen and its value is typically obtained from the phenotypic ASTs after overnight incubation.[30] Because the MIC results are usually obtained from individual homogeneous bacteria traditionally

cultivated in their planktonic form, they cannot be used as a clinical breakpoint to treat biofilm-related infections.[17] The energy calculated from the metabolic EET of the biofilm formed in the paper culturing platform can provide a rapid determination of the antibiotic MIC before the cellular growth and reproduction are visually monitored through a long culture-based technique.

To precisely quantify the energy plateaus and determine the MICs, all energy curves for antibiotic-susceptible *P. aeruginosa* were converted to slopes that were re-plotted in Figure 5. The slope, *S*, was calculated in the following,

$$S = \frac{E_{t+1} - E_{t-1}}{(t+1) - (t-1)} \quad (2)$$

where *t* is the time (x-axis) and *E* is the energy (y-axis) in micro-Jules from Figures 2, 3, and 4. Figure 5 shows the calculated slopes over time for (a) GEM-susceptible, (b) CIP-susceptible, and (c) AMP-susceptible *P. aeruginosa.* When the energy reaches a plateau, the slope decreases to zero. To provide further comparison, bar graphs of the time required to reach zero slope are included in Supplementary Figure S1. The MIC value of the antibiotic depends on the cell density in a biofilm (Table S7). The energy slope of the highest cell densities at 1.0 OD_{600} never became zero against all antibiotics that we used. Therefore, it will be clinically important to obtain the MICs according to the actual pathogen concentration on the infected sites.

2.4 Electrical signatures of action mechanisms for antibiotics. Throughout this work, we used three antibiotics having distinct mechanisms of action: gentamicin (protein synthesis), ciprofloxacin (DNA transcription), and ampicillin (cell wall synthesis).[31] From Figure 5, the steepness, the onset of the zero slope, and the decreasing trend revealed the action

mechanisms of those antibiotics. Gentamicin belongs to the aminoglycosides antibiotic family that binds to the 30S subunit of the ribosome, inhibiting protein synthesis. For gentamicin-susceptible bacterial samples, the slope curve at the initial stage had a gradual drop after the addition of gentamicin but it decreased sharply to zero at a later stage, demonstrating two distinct decreasing phases (Figure 5a). This possibly represents two general steps of gentamicin against bacteria; binding and inhibition.

On the other hand, ciprofloxacin belongs to the class of fluoroquinolone antibiotics that can inhibit DNA transcription and replication. The slope curves for ciprofloxacin-susceptible *P. aeruginosa* showed a one-step gradual decrease, slowly inhibiting bacterial metabolism and growth (Figure 5b). The onsets of the zero slopes were generally delayed compared to the gentamicin counterparts, indicating that ciprofloxacin is less effective than gentamicin against *P. aeruginosa* biofilms.

Ampicillin is a penicillin beta-lactam antibiotic that can lyse bacterial cells by preventing cell wall synthesis. While it is well-known that *P. aeruginosa* is 100% resistant to ampicillin, the data shows that its high concentration of 100μg/mL is weakly effective against a biofilm three-dimensionally formed with a lower bacterial density at 0.1 OD_{600}. However, given that the slope profile and value are almost the same as the control without the antibiotic and the onset of the zero slope appears at the last stage of the measurement (~ 4000 s) (Figure 5c), it does not look like the action mechanism of ampicillin is properly working.

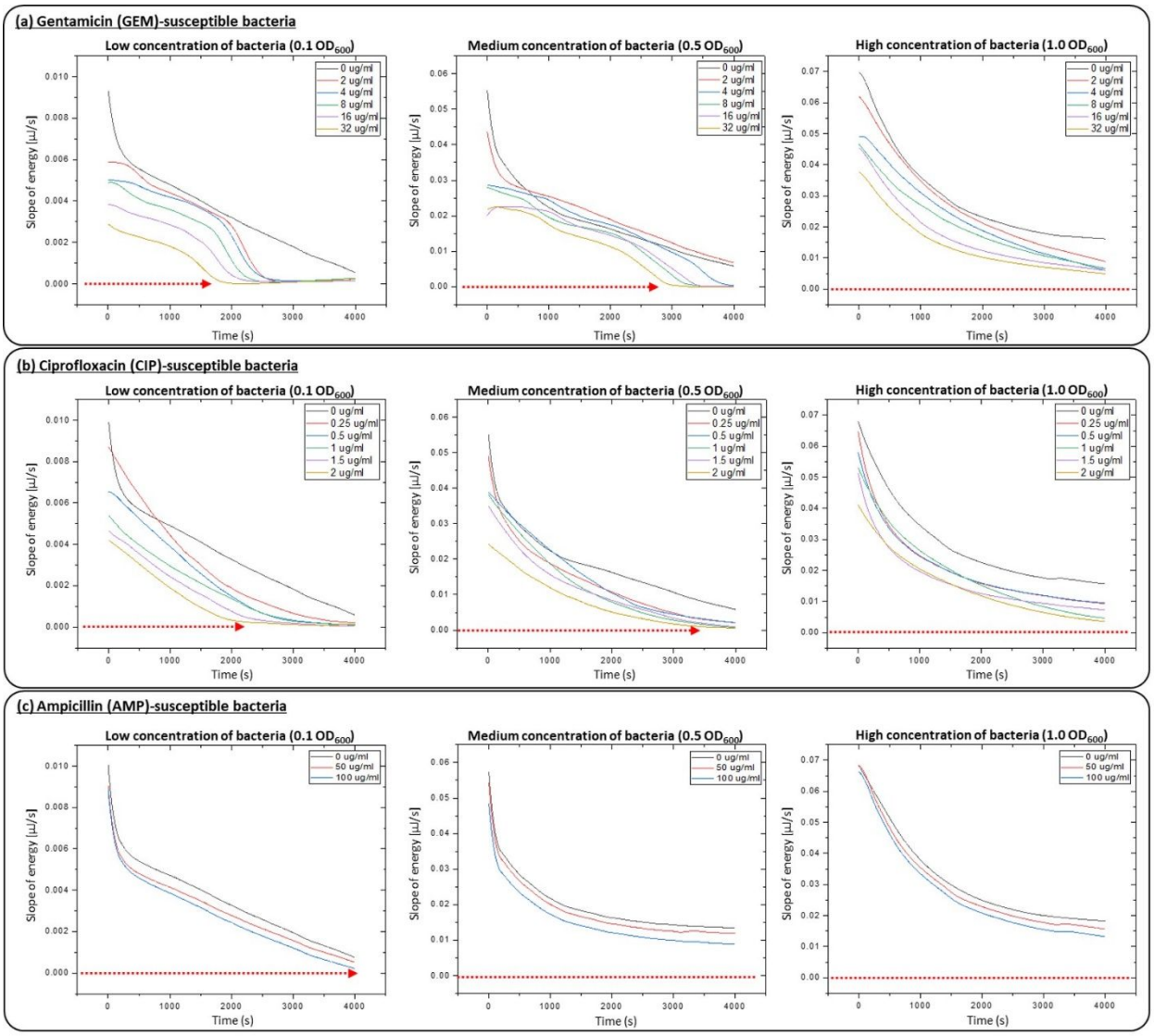

Figure 5. Slope of the energy curves of antibiotic-susceptiable *P. aeruginosa.* The energy slope is caculated from Figures 2, 3, and 4 in micro-jules/s. (a) Gentamicin-susceptable *P. aeruginosa,* (b) Ciprofloxacin-susceptable *P. aeruginosa,* (c) Ampicillin-susceptable *P. aeruginosa.* When the antibiotic is effective, the slope becomes zero indicating the onset of the termination of bcaterial metabolic activity and growth.

3. Future direction

Although more studies show that many clinical pathogens can be identified by their EET activities, still some pathogens can be hardly detected in the proposed AST device. However, by exogenously dosing redox mediators, the electrons from those pathogens can be extracellularly transferred to the outside sensing electrode. Further studies with non-

exoelectrogenic pathogens are needed. Moreover, exploring the use of patient-derived clinical isolates instead of laboratory strains may further enhance the platform's applicability to clinical settings. These directions hold tremendous potential for advancing the use of the 3-D paper-based culture platform for AST and improving its utility in clinical practice.

4. Conclusion

Here, we created an innovative AST technique specific to biofilms that offers clinically relevant guidelines. Our approach was based on a paper-based 3-D cell culture platform that recapitulated the structure, function, and physiology of *P. aeruginosa* biofilms and simultaneously monitored bacterial EET that directly reflected bacterial viability and metabolism. The EET allowed a rapid phenotypic evaluation of antibiotic effectiveness much quicker than traditional culture-based techniques that require clinicians to count the number of cells before and after the considered treatment. Our device allowed clinicians to assess within 100 minutes (30 minutes for waiting and 67 minutes for the EET measurement) whether an antibiotic worked against a biofilm-protected infection. We successfully distinguished antibiotic-susceptible and -resistant *P. aeruginosa* biofilms, quantified the MICs and differentiated antibiotic action mechanisms. Our AST device will become a practical point-of-care tool that provides immediately actionable healthcare information at a reduced cost, revolutionizing public healthcare in developed and developing countries. Furthermore, this technique will enable a versatile platform for fundamental studies of antibiotic resistance.

Materials and methods

Fabrication of the AST array The AST array was constructed by two folds of the 2-D paper sheet (Whatman Grade 3MM Chr Chromatography paper) that had integrated three functional tabs; (i) antibiotic layer, (ii) anode layer, and (iii) cathode layer with an ion-exchange membrane (Figure 1b and S2). The 2-D paper sheet was prepared by double-sided wax printing (ColorQube 8570), heat-treatment for the wax penetration (at 150 °C for 50 seconds), and laser dicing (Universal Laser System VLS 3.5). The hydrophobic wax boundaries defined six antibiotic wells, anodic chambers, and cathodic areas while the asymmetrically penetrated wax served as the ion-exchange membrane when the anodic and cathodic layers were put together by folding. T The antibiotic layer was prepared with six different concentrations of antibiotics and each concentration was signified by the intensity of the blue in the wax used to separate the components. The anodic and cathodic regions were first conductively engineered with PEDOT:PSS (Clevios PH1000, Heraeus) and dimethyl sulfoxide (DMSO, Sigma Aldrich), followed by screen-printing graphite ink (E3449, Ercon) as an electron collector. The cathodic part was additionally treated with Ag_2O for the cathodic reduction process. More fabrication details are available in our previous reports.[27]

Bacterial sample preparation *P. aeruginosa* PAO1 was used as a model electrogenic pathogen. *P. aeruginosa* from -80°C glycerol stock was cultured in a LB medium for about 5 hours at 37°C to an OD_{600} of 1.0, followed by centrifugal separation of the supernatant. The pellet was resuspended in a new LB medium and diluted to prepare three samples with 0.1, 0.5, and 1.0 OD_{600}. Antibiotic-resistant *P. aeruginosa* was obtained by repeatedly exposing the bacteria to low concentrations of each antibiotic, GEM, CIP, and AMP,[32] and

their resistance was confirmed by the disk diffusion test (Figure S3). This *in vitro* experimental evolution of bacteria to antibiotics has been commonly used to identify the mechanisms of antibiotic resistance.[32,33]

Preparation of the antibiotics We selected three antibiotics with distinct action mechanisms. GEM, CIP, and AMP belong to aminoglycoside, fluoroquinolones, and β-lactam families, respectively.[31] GEM interferes with protein synthesis while CIP blocks bacterial DNA replication and AMP inhibits cell wall synthesis. A diluted series of antibiotics were made to quantify the MIC values according to different bacterial concentrations. The GEM was prepared in six dilutions; 0 μg/ml, 2 μg/ml, 4 μg/ml, 8 μg/ml, 16 μg/ml, and 32 μg/ml while the CIP was 0 μg/ml, 0.25 μg/ml, 0.5 μg/ml, 1 μg/ml, 1.5 μg/ml, 2 μg/ml in sterile LB. The AMP was prepared in three dilutions; 0 μg/ml, 50 μg/ml, and 100 μg/ml. The antibiotic layer was loaded with the different concentrations of each antibiotic and air-dried, which allowed easy-to-test and rapid AST with a one-step dropping of a bacterial sample.

AST procedures 10μL of each bacterial sample of 0.1, 0.5, and 1.0 OD_{600} was introduced into each AST array housing antibiotics in different concentrations. The sample was absorbed by the antibiotic well (5μL volume) first and then transported to the anodic chamber (5μL volume). After the sample loading, we waited for 30 minutes to ensure the complete mixing of bacteria and the antibiotic and allow the cells to accumulate on the anode. The accumulated power over time (with an external resistor of 47.5 kΩ) was continuously monitored with a data acquisition system (DI-4108U, DataQ). The maximum power of the microbial fuel cell was obtained from the external resistor.

Broth microdilution (BMD) The gold standard broth microdilution (BMD) was used to compare our MIC values. The BMD protocol was based on the Clinical and Laboratory Standards Institute (CLSI) guidelines.[28]

Statistical analysis All experimental data shown in this work were performed by repeating identical experiments at least three times. Data were represented as the mean ± standard errors of those experimental replicates.

Acknowledgments

This work was supported partially by the National Science Foundation (CBET #2100757).

References

1. F. Balloux, L. van Dorp, Q&A: What are pathogens, and what have they done to and for us?, *BMC Biol.*, 2017, **15**, 91.
2. P. Swami, A. Sharma, S. Anand, S. Gupta, DEPIS: A combined dielectrophoresis and impedance spectroscopy platform for rapid cell viability and antimicrobial susceptibility analysis, *Biosens. Bioelectron.*, 2021, **182**, 113190.
3. Nature Editorial, Microbiology by numbers, *Nat. Rev. Microbiol.*, 2011, **9**, 628,
4. M.I. Hutchings, A.W. Truman, B. Wilkinson, Antibiotics: past, present and future, *Curr. Opin. Microbiol.*, 2019, **51**, 72-80.
5. J.H. Kwon, W.G. Powderly, The post-antibiotic era is here, *Science*, 2021, **373**, 471.
6. C. Llor, L. Bjerrum, Antimicrobial resistance: risk associated with antibiotic overuse and initiatives to reduce the problem, *Ther Adv Drug Saf.*, 2014, **5**, 229-241.
7. C.L.M. de Opitz, P. Sass, Tackling antimicrobial resistance by exploring new mechanisms of antibiotic action, *Future Microbiology*, 2020, **15**, 703-708.

8. Nature Editorial, Wanted: a reward for antibiotic development, *Nat. Biotechnol.*, 2018, **36**, 555.

9. E.A. Idelevich, K. Becker, How to accelerate antimicrobial susceptibility testing, *Clin. Microbiol. Infect.*,2019, **25**, 1347-1355.

10. M.A. Hudson, S.W. Lockless, Elucidating the mechanisms of action of antimicrobial agents, *mBio*, 2022, **13**, 02240-21.

11. B. Behera, A. Vishnu, S. Chatterjee, V.S.N. Sitaramgupta, N. Sreekumar, A. Nagabhushan, N. Rajendran, B.H. Prathik, H.J. Panday, Emerging technologies for antibiotic susceptibility testing, *Biosens. Bioelectron.*, 2019, **142**, 111552.

12. H. Leonard, R. Colodner, S. Halachmi, E. Segal, Recent advances in the race to design a rapid diagnostic test for antimicrobial resistance, *ACS Sensors*, 2018, **3**, 2202-2217.

13. D.J. Shin, N. Andini, K. Hsieh, S. Yang, T. Wang, Emerging analytical techniques for rapid pathogen identification and susceptibility testing, *Annu. Rev. Anal. Chem.*, 2019, **12**, 41-67.

14. R.K. Shanmugakani, B. Srinivasan, M.J. Glesby, L.F. Westblade, W.B. Cardenas, T. Raj, D. Erickson, S. Mehta, Current state of the art in rapid diagnostics for antimicrobial resistance, *Lab Chip*, 2020, **20**, 2607-2625.

15. A. Mezger, E. Gullberg, J. Goransson, A. Zorzet, D. Herthnek, E. Tano, M. Nilsson, D.I. Andersson, A General Method for Rapid Determination of Antibiotic Susceptibility and Species in Bacterial Infections, *J. Clin. Microbiol.*, 2015, **53**, 425.

16. A. Penesyan, I.T. Paulsen, M.R. Gillings, S. Kjelleberg, M.J. Manefield, Secondary effects of antibiotics on microbial biofilms, *Front. Microbiol*., 2020, **11**, 2109.

17. M. Jamal, W. Ahmad, S. Andleeb, F. Jalil, M. Imran, M.A. Nawaz, T. Hussain, M. Ali, M. Rafiq, M.A. Kamil, Bacterial biofilm and associated infections, *J. Chin. Med. Assoc*., 2018, **81**, 7-11.

18. A. Kumar, A. Alam, M. Rani, N.Z. Ehtesham, S.E. Hasnain, Biofilm: survival and defense strategy for pathogens, *Int. J. Med. Microbiol*., 2017, **307**, 481-489.

19. Z. Rafiee, M. Rezaie, S. Choi, Accelerated antibiotic susceptibility testing of Pseudomonas aeruginosa by monitoring extracellular electron transfer on a 3-D paper-based cell culture platform, *Biosens. Bioelectron.*, 2022, **216**, 114604.

20. Y. Gao, J. Ryu, L. Liu, S. Choi, A simple, inexpensive, and rapid method to assess antibiotic effectiveness against exoelectrogenic bacteria, *Biosens. Bioelectron.*, 2020, **168**, 112518.

21. G. Reguera, Biological electron transport goes the extra mile, *PNAS*, 2018, **115**, 5632-5634.

22. D.R. Lovley, Electromicrobiology, *Annu. Rev. Microbiol.*, 2012, **66**, 391-409.

23. S. Choi, Electrogenic Bacteria Promise New Opportunities for Powering, Sensing, and Synthesizing, *Small,* 2022, **18**, 2107902.

24. K. Aiyer, L.E. Doyle, Capturing the signal of weak electricigens: a worthy endeavor, *Trends Biotechnol*., 2022, **40**, 564.

25. G. Tibbits, A. Mohamed, D.R. Call, H. Beyenal, Rapid differentiation of antibiotic-susceptible and -resistant bacteria through mediated extracellular electron transfer, *Biosens. Bioelectron.*, 2022, **197**, 113754.

26. A. Elhadad, S. Choi, Biofabrication and Characterization of Multispecies Electroactive Biofilms in Stratified Paper-based Scaffolds, *Analyst*, 2022, **147**, 4082-4091.

27. M. Tahernia, M. Mohammadifar, Y. Gao, W. Panmanee, D.J. Hassett, S. Choi, A 96-well high-throughput, rapid-screening platform of extracellular electron transfer in microbial fuel cells, *Biosens. Bioelectron.*, 2022, **162**, 112259.

28. I. Wiegand, K. Hilpert, R.E.W. Hancock, Agar and broth dilution methods to determine the minimal inhibitory concentration (MIC) of antimicrobial substances, *Nat. Protoc.*, 2008, **3**, 163-175.

29. S.T. Alam, T.A.N. Le, J. Park, H.C. Kwon, K. Kang, Antimicrobial Biophotonic Treatment of Ampicillin-Resistant Pseudomonas aeruginosa with Hypericin and Ampicillin Cotreatment Followed by Orange Light, *Pharmaceutics*, 2019, **11**, 641.

30. J.M. Andrews,Determination of minimum inhibitory concentrations, *J. Antimicrob. Chemother.*, 2001, **48**, Suppl. 1:5-16.

31. A. E. Garima Kapoor, Saurabh Saigal1, Action and resistance mechanisms of antibiotics: A guide for clinicians, *J. Anaesthesiol. Clin. Pharmacol.*, 2018, **34**, 46–50.

32. T. Coenye, M. Bove, T. Bjarnsholt, Biofilm antimicrobial susceptibility through an experimental evolutionary lens, *npj biofilms and microbiomes*, 2022, **8**, 82.

33. S. Seo, S. Disney-Mckeethen, R.G. Prabhakar, X. Song, H.H. Mehta, Y. Shamoo, Identification of evolutionary trajectories associated with antimicrobial resistance using microfluidics, *ACS Infect. Dis.*, 2022, **8**, 242-254.